Electronic Supplementary Information to:

Molecular Ordering-Enhanced Circularly Polarized Luminescence of Chiral 1,10-Phenanthroline Derivatives

Masayoshi Bando,[a] Mariagrazia Fortino,[b] Adriana Pietropaolo,[b] Yukatsu Shichibu,[c] Katsuaki Konishi,[c] and Tamaki Nakano[a,d,*]

[a]Institute for Catalysis (ICAT), Hokkaido University, N21W10, Kita-ku, Sapporo 001-0021, Japan

[b]Dipartimento di Scienze della Salute, Università di Catanzaro, Catanzaro, Italy

[c]Faculty of Environmental Earth Sciences, Hokkaido University, N10 W5, Kita-ku, Sapporo, Hokkaido 060-0810, Japan

[d]Integrated Research Consortium on Chemical Sciences (IRCCS), Institute for Catalysis, Hokkaido University, N21 W10, Kita-ku, Sapporo, Hokkaido 001-0021, Japan

*tamaki.nakano@cat.hokudai.ac.jp

Table of Contents

Experimental

Materials. 1,10-phenanthroline monohydrate (TCI), 1,3-dibromopropane (TCI), nitrobenzene (Wako), potassium *tert*-butoxide (TCI), *tert*-butyl alcohol (Kanto), phosphorus(V) chloride (Kanto), phosphoryl chloride (Nacalai), (1R,2S,5R)-menthol (Wako), (1S,2R,5S)-menthol (TCI), (S)-(-)-2-methyl-1-butanol (TCI), N,N-dimethylformamide (DMF) (Nacalai), sodium hydride (TCI), chloroform (Kanto), chloroform-d_1 (Kanto) and Silica-gel 60 N (neutral) (Kanto) were used as purchased. Tetrahydrofuran (THF) (Wako) was dried on calcium hydride under nitrogen flow.

General instrumentation. ^{1}H NMR spectra were recorded on a JEOL JNM-ECX400 spectrometer (400 MHz for ^{1}H measurement) and a JEOL JNM-ECA600 spectrometer (600 MHz for ^{1}H measurement). UV-vis absorption spectra were measured at room temperature with a JASCO V-570 spectrophotometers. Steady-state emission spectra were taken on a JASCO FP-8500 fluorescence spectrophotometer. Emission quantum yield was determined by measurements using a JASCO ILF-835 integrating sphere. Emission lifetime (τ) was measured on a Hamamatsu Photonics Quantaurus Tau fluorescence lifetime-transient absorption analysis system. Circular dichroism (CD) spectra were taken with a JASCO-820 spectrometer. The spectra of films were obtained by averaging those recorded at four different film orientations (angles) at an interval of 90° with the film face positioned orthogonally to the incident light beam for measurement. The anisotropy factor (g_{CD}) was calculated according to $g_{CD} = \Delta Abs/Abs = (\text{ellipticity}/32980)/Abs$. CPL spectra were measured with an assembled apparatus based on a photo elastic modulator and a photomultiplier designed according to the literature[1] with modifications. The emission anisotropy factor (g_{lum}) was calculated according to $g_{lum} = 2(I_L - I_R)/(I_L + I_R)$ where I_L and I_R are the emission intensities of L- and R-CPL, respectively. The spectra of films were obtained by averaging those recorded at two different film angles that are different by 90° with the film face positioned orthogonally to the incident light beam for measurement where excitation was conducted from the back side and the front side.

Crystal structure analysis. Crystal data were collected on a Rigaku XtaLAB P200 diffractometer with a multi-mirror monochromated Cu K_α radiation ($\lambda = 1.54184$ Å) at 100 K. The crystal structure was solved by intrinsic phasing method (SHELXT-2018)[2] and refined by full-matrix least-squares methods on F^2 (SHELXL-2018)[3] with Olex2 software.[4] All non-hydrogen atoms were refined anisotropically, and the hydrogen atoms were refined isotropically. Crystal data for **Men2Phen**·$C_{32}H_{44}N_2O_2$; $M = 488.69$; $0.23 \times 0.12 \times 0.08$ mm^3; orthorhombic; space group $P2_12_12_1$ (no. 19); $a = 8.79630(10)$ Å, $b = 9.51980(10)$ Å, $c = 34.7853(4)$ Å; $V = 2912.89(6)$ Å^3; $Z = 4$; $\rho_{calcd} = 1.114$ gcm^{-3}; $\mu = 0.530$ mm^{-1}; $\theta_{max} = 72.284°$; reflections collected: 10039, independent reflections: 5380 ($R_{int} = 0.0241$), $R_1(I{>}2\sigma) = 0.0318$, $wR_2(I{>}2\sigma) = 0.0863$; final difference map within +0.194 and –0.143 eÅ^3. CCDC-2255081 (**Men2Phen**) contains the

supplementary crystallographic data for this paper. These data can be obtained free of charge from The Cambridge Crystallographic Data Centre via www.ccdc.cam.ac.uk/data_request/cif.
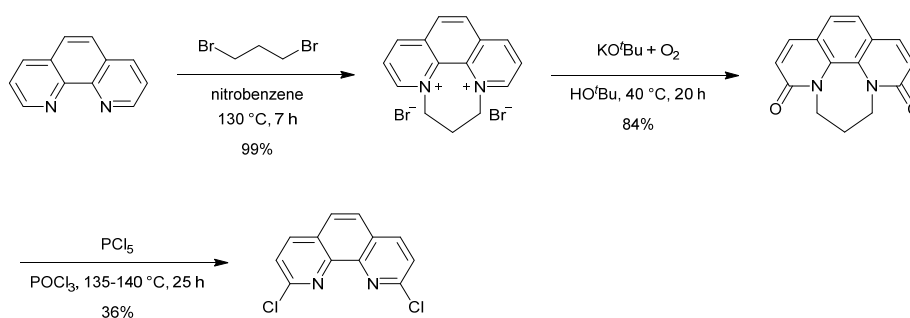
2,9-Dichloro-1,10-phenanthroline. This compound was synthesized according to the literature with modifications (Scheme S1).[5]

To a 1-L two-neck round-bottom flask equipped with a glass stopper and a reflux condenser to which a three-way stopcock was attached as a nitrogen inlet were added 1,10-phenanthroline monohydrate (45.1 g, 227 mmol), nitrobenzene (380 mL) and 1,3-dibromopropane (130 mL, 1.27 mol) under nitrogen. The mixture was stirred with a stirring bar and a magnetic stirrer at 130 °C for 7 h, and was then cooled to room temperature. The quaternary salt was obtained as yellow precipitates which were collected by filtration, washed with hexane, and dried under reduced pressure for 12 h. Yield 86.1 g, 225 mmol, 99%.

To a 2-L round-bottom flask were added the quaternary salt (45.5 g, 119 mmol), *tert*-butyl alcohol (680 mL), and potassium *tert*-butoxide (56.1 g, 500 mmol). The mixture was stirred at 40 °C for 20 hours under air, and oxygen was bubbled through it for 1 h. The solvent was removed under reduced pressure, and water and $CHCl_3$ were added to the residue. The $CHCl_3$ layer was washed with brine, dried over anhydrous $MgSO_4$, filtered, and concentrated to give a raw product of the dione compound. The product was used for the next reaction without further purification. Yield 25.3 g, 100 mmol, 84%.

To a 1-L two-neck round-bottom flask equipped with a glass stopper and a reflux condenser to which a three-way stopcock was attached as a nitrogen inlet were added the dione (18.9 g, 75 mmol), phosphorus(V) chloride (31.3 g, 150 mmol), and phosphoryl chloride (300 mL) under nitrogen. The mixture was stirred at 135-140 °C for 25 hours, and was then cooled to room temperature. After the removal of remaining phosphoryl chloride under reduced pressure, 1 M aqueous ammonia was added to the residue to neutralize the mixture. The products were extracted with dichloromethane, washed with brine, dried over anhydrous $MgSO_4$, and concentrated. The residue was purified by column chromatography (silica gel, dichloromethane as eluent) to give 2,9-dichloro-1,10-phenanthroline as brown solid (6.7 g, 26.7 mmol, 36%).

^{1}H NMR (600 MHz, $CDCl_3$) δ 8.22 (d, *J* = 8.2 Hz, 2H), 7.83 (s, 2H), 7.65 (d, *J* = 8.2 Hz, 2H); ^{13}C NMR (150 MHz, $CDCl_3$) δ 152.1, 145.1, 138.9, 127.9, 126.4, 125.1.

Scheme S1. Synthesis of 2,9-dichloro-1,10-phenanthroline.

2,9-Bis(((1*R*,2*S*,5*R*)-2-isopropyl-5-methylcyclohexanoxy)-1,10-phenanthroline [2,9-Di-*l*-menthoxy-1,10-phenanthroline] (1) (Scheme S2). To a 200-mL two-neck round-bottom flask equipped with a rubber septum and a three-way stopcock were added NaH (60%, dispersion in paraffin liquid, 1.56 g, 39 mmol), dried DMF (80 mL) and *l*-(-)-menthol (2.75 g, 17.6 mmol) in this order under N_2 atmosphere. After stirring at room temperature for 30 min, 2,9-dichloro-1,10-phenanthroline (1.99 g, 8 mmol) was added to the mixture. The reaction was conducted at 100 ºC for 12 h with stirring. The mixture was then cooled to room temperature and added carefully to excess H_2O. The products were extracted with $CHCl_3$, washed with H_2O, dried over anhydrous Na_2SO_4, and concentrated. The residue was purified by column chromatography (silica gel, hexane-$CHCl_3$ (5/1, v/v) as eluent) to give compound **1** as white solid (1.87 g, 3.83 mmol, 48%).

^{1}H NMR (600 MHz, $CDCl_3$) δ 8.02 (d, *J* = 8.6 Hz, 2H), 7.54 (s, 2H), 6.99 (d, *J* = 8.9 Hz, 2H), 5.83-5.73 (m, 2H), 2.45-2.35 (m, 2H), 2.19-2.09 (m, 2H), 1.87-1.77 (m, 4H), 1.77-1.68 (m, 2H), 1.67-1.59 (m, 2H), 1.28-1.18 (m, 2H), 1.14-1.06 (m, 2H), 1.06-0.98 (m, 2H), 0.96 (d, *J* = 6.9 Hz, 6H), 0.95 (d, *J* = 6.5 Hz, 6H), 0.87 (d, *J* = 6.9 Hz, 6H); ^{13}C NMR (150 MHz, $CDCl_3$) δ 162.0, 143.7, 138.7, 125.0, 123.0, 113.7, 74.4, 47.9, 40.9, 34.9, 32.1, 26.5, 24.1, 22.4, 21.1, 16.9. HRMS(EI) Calcd. for $C_{32}H_{44}N_2O_2$: 488.34028. Found: 488.34000.
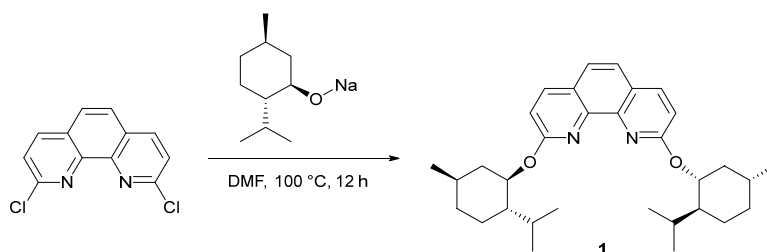

Scheme S2. Synthesis of 2,9-bis(((1*R*,2*S*,5*R*)-2-isopropyl-5-methylcyclohexanoxy)-1,10-phenanthroline (1).

2,9-Bis(((1*S*,2*R*,5*S*)-2-isopropyl-5-methylcyclohexanoxy)-1,10-phenanthroline [2,9-Di-d-menthoxy-1,10-phenanthroline] To a 100-mL two-neck round-bottom flask equipped with a rubber septum, a three-way stopcock and a stirring bar were added NaH (60%, dispersion in paraffin liquid, 470 mg, 11.7 mmol), dried DMF (24 mL) and *d*-(+)-menthol (830 mg, 5.3 mmol) in this order under N_2 atmosphere. After stirring at room temperature for 30 min, 2,9-dichloro-1,10-phenanthroline (600 mg, 2.4 mmol) was added to the mixture. The mixture was stirred at 100 ºC for 12 hours. The mixture was then cooled to room temperature and added carefully to excess H_2O. The products were extracted with $CHCl_3$, washed with H_2O, dried over anhydrous Na_2SO_4, and concentrated. The residue was purified by column chromatography (silica gel, hexane-$CHCl_3$ (3/1, v/v) as eluent) to give the target compound as white solid (600 mg, 1.2 mmol, 51%).

^{1}H NMR (400 MHz, $CDCl_3$) δ 8.01 (d, J = 8.6 Hz, 2H), 7.53 (s, 2H), 6.98 (d, J = 8.6 Hz, 2H), 5.82-5.72 (m, 2H), 2.44-2.34 (m, 2H), 2.19-2.06 (m, 2H), 1.87-1.76 (m, 4H), 1.76-1.67 (m, 2H), 1.67-1.58 (m, 2H), 1.28-1.15 (m, 2H), 1.15-0.98 (m, 4H), 0.98-0.89 (m, 12H), 0.85 (d, J = 7.0 Hz, 6H); ^{13}C NMR (100 MHz, $CDCl_3$) δ 162.0, 143.6, 138.7, 125.0, 123.0, 113.7, 74.4, 47.9, 40.9, 34.9, 32.1, 26.5, 24.0, 22.4, 21.0, 16.9.

2,9-Bis[(*S*)-(-)-2-methyl-1-butoxy]-1,10-phenanthroline (2) (Scheme S3). To a 200-mL two-neck round-bottom flask equipped with a rubber septum and a three-way stopcock were added NaH (60%, dispersion in paraffin liquid, 1.56 g, 39 mmol), dried DMF (80 mL) and (*S*)-(-)-2-methyl-1-butanol (1.9 mL, 17.6 mmol) in this order under N_2 atmosphere. After stirring at room temperature for 30 min, 2,9-dichloro-1,10-phenanthroline (1.99 g, 8 mmol) was added to the mixture. The mixture was stirred at room temperature for additional 12 h, and was then added carefully to excess H_2O. The products were extracted with $CHCl_3$, washed with H_2O, dried over anhydrous Na_2SO_4, and concentrated. The residue was purified by column chromatography (alumina activated, hexane-$CHCl_3$ (3/1, v/v) containing 2% triethylamine as eluent) to give compound **2** as brown oil (2.59 g, 7.35 mmol, 92%).

^{1}H NMR (400 MHz, $CDCl_3$) δ 8.07 (d, J = 8.8 Hz, 2H), 7.59 (s, 2H), 7.06 (d, J = 8.6 Hz, 2H), 4.61 (dd, J = 10.6, 6.1 Hz, 2H), 4.48 (dd, J = 10.4, 7.0 Hz, 2H), 2.11-1.99 (m, 2H), 1.70-1.59 (m, 2H), 1.41-1.30 (m, 2H), 1.09 (d, J = 6.8 Hz, 6H), 1.01 (t, J = 7.5 Hz, 6H); ^{13}C NMR (100 MHz, $CDCl_3$) δ 162.9, 143.2, 139.0, 125.2, 123.3, 113.7, 71.0, 34.5, 26.5, 16.8, 11.5. HRMS(EI) Calcd for $C_{22}H_{28}N_2O_2$: 352.21508. Found: 352.21501.
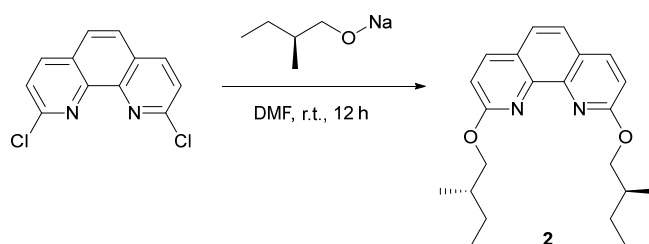
Scheme S3. Synthesis of 2,9-bis[(*S*)-(-)-2-methyl-1-butoxy]-1,10-phenanthroline (**2**).

Film preparation. Film samples were prepared by the following procedure. Polymer (about 1 mg) was dissolved in 1,4-dioxane (0.3-0.5 mL), and an aliquot (ca. 0.05 mL) of the solution was dropped onto a 1-mm quartz plate (1cm x 2 cm x 1 mm) and dried under air at r.t.

Computational method. Structural optimization in the ground state corresponding to the results in Figure 4 in the main text and in Fig. S1 was conducted at wB97xD/6-31G(d) level using Gaussian16.[6] Geometries including dihedral angles of the optimized conformation were analyzed using Discover Studio Visualizer (Dassault Systèmes).

All the simulations regarding the results in Figure 6 in the main text have been carried out by using the unitary cell containing four **chiral Phen 1** molecules distributed following the helix pitch.

Ab-initio molecular dynamics (AIMD) were performed in the S0 ground state to sample the configurations to predict the absorption UV-vis and ECD spectra. The hybrid Gaussian and plane waves method (GPW) as implemented in the QuickStep module of the CP2K package has been used.[7] The control of the temperature has been implemented by using Nosè-Hoover thermostats[8,9] with a temperature of 300 K. The electronics structure properties have been computed by using PBE as density functional with the Grimme D3 corrections[10] to account for the dispersion interactions. Kohn-Sham orbitals have been expanded in DZVP-GTH Gaussian basis sets and the norm-conserving GTH pseudopotentials have been employed for all atoms.

The auxiliary plane wave (PW) basis set was defined by the energy cutoff of 400 Ry. The time set of the integration of the dynamics equations was set to 1fs. The ab-initio molecular dynamics simulation in S0 has been extended up to 3 ps. Configurations has been extracted from the computed S0 AIMD trajectory and used for the simulations of the absorption UV-vis and ECD spectra, following the simulation workflows reported in[10,11] to predict chiroptical properties. The excitation energies, oscillator strengths and rotatory strengths have been computed for the coordinates selected from the ab initio trajectories at the wb97xd/6-31G level of theory, with the Gaussian16 software. The calculations of the UV-vis and ECD spectra at a given excitation wavelength have been carried out assuming Gaussian bands with a full width at half-height of

350 cm^{-1} for all transitions. A shift of 20 nm has been applied to match the experiments.

PL and CPL spectra simulations were derived from the AIMD simulation in the first excited state S1 with a total simulation time of 3 ps, by maintaining the same computational protocol described for the S0 AIMD simulation. The configurations were extracted from the AIMD trajectory in the S1 state and used for the simulations of the absorption UV-vis and ECD spectra. The oscillator strengths and rotatory strengths have been computed at wB97xD/6-31G level of theory, by using Gaussian16 as software.

PL and CPL intensities (I and ΔI, respectively) are derived by using the following expressions, as also described in[11-14]:

$$I = \frac{4E^3 \rho(E)D_{01}}{3\hbar^4 c^3} = 1.27 \cdot 10^{-7}E^3\rho(E)D_{01} \qquad (1)$$

$$\Delta I = \frac{16E^3 \rho(E)R_{01}}{3\hbar^4 c^3} = 5.09 \cdot 10^{-13}E^3\rho(E)R_{01} \qquad (2)$$

Where D_{01} and R_{01} are the dipole and rotational strengths, respectively, associated to the transition 0-1, E is the emission energy of the given transition expressed in cm^{-1}, $\rho(E)$ is a Gaussian band shape and the calculated constants are coherently expressed in cgs units. The PL and CPL intensities have been then normalized to arbitrary relative units by assuming Gaussian bands with 600 cm^{-1} full width at half-height for all transitions in a given emission energy. A shift of 20 nm has been applied.
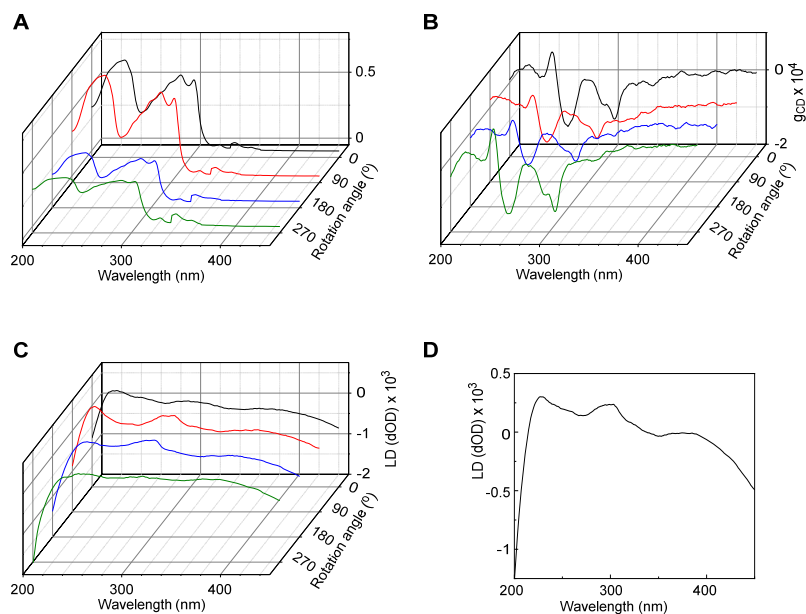
The emission dissymmetry factor (g$_{lum}$) has been calculated by using equation 3:

$$g_{lum} = \frac{4R_{01}}{D_{01}} \qquad (3)$$
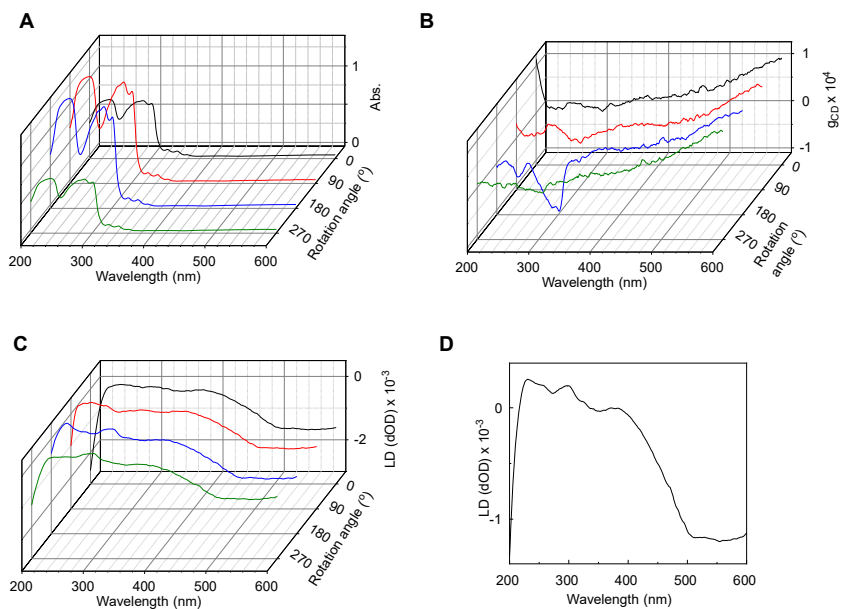
A. 1

B. 2

C. Phen
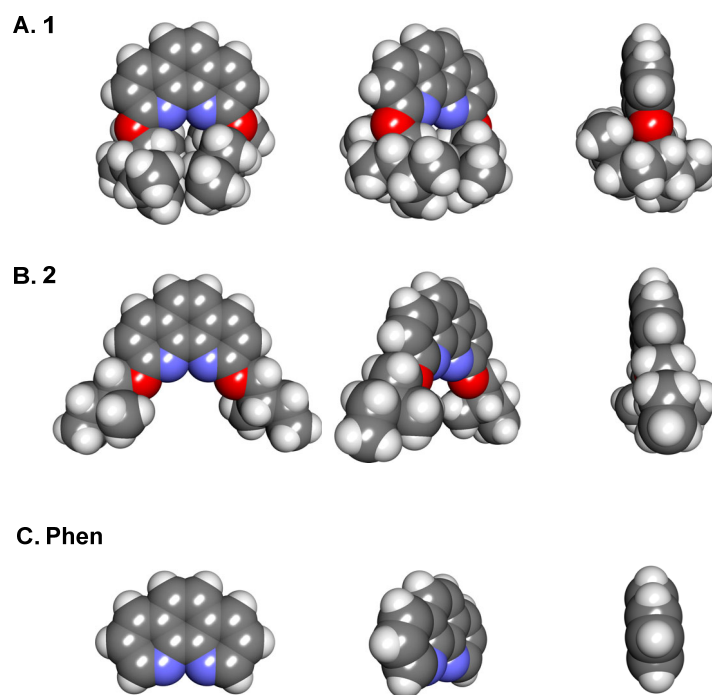
Fig. S1. DFT-optimized structures of **1** (A), **2** (B), and **Phen** (C) viewed from different angles. [DFT conditions: wB97xD/6-31G(d)]

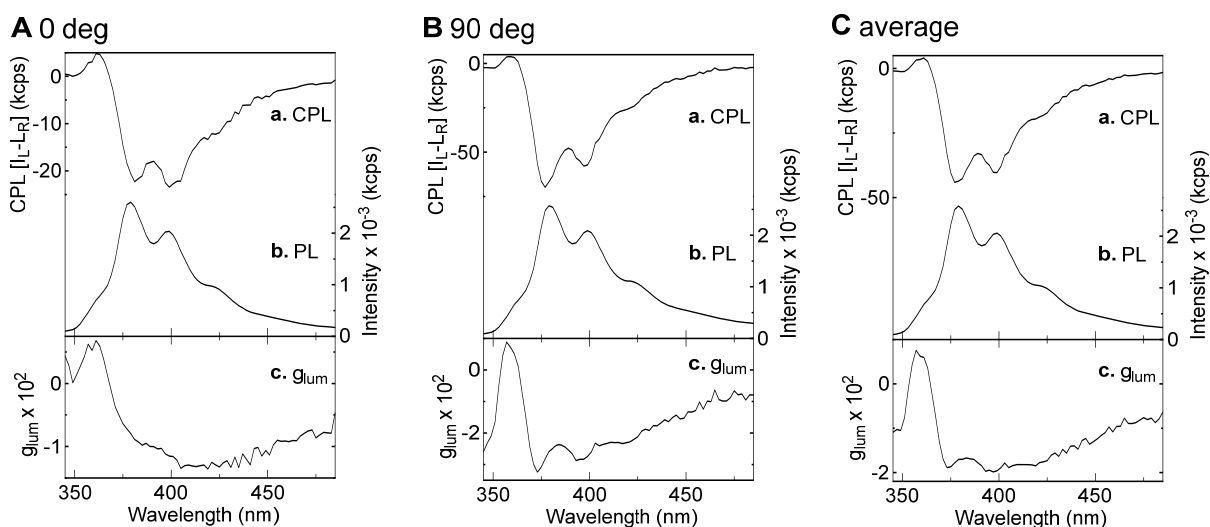**Fig. S2.** Absorbance (A), g_{CD} (B), and LD (C) spectra of **Men2Phen** film measured at four different angles (0, 90, 180, and 270 degrees) and averaged LD spectrum (D).
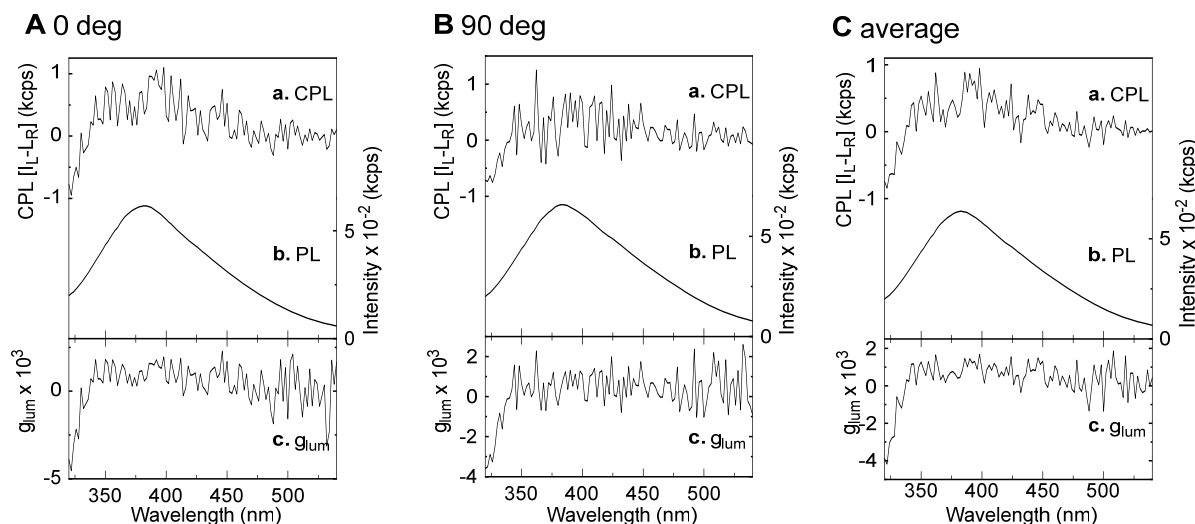

Fig. S3. Absorbance (A), g_{CD} (B), and LD (C) spectra of **MB2Phen** film measured at four different angles (0, 90, 180, and 270 degrees) and averaged LD spectrum (D).

Fig. S4. CPL (a), PL (b), and g$_{lum}$ (c) spectra of **Men2Phen** film measured at 0 degrees (A) and 90 degrees (B) of the sample by irradiating the film from the *back side* of the sample and those obtained by averaging the spectra in A and B (C). [λ$_{ex}$ 260 nm]
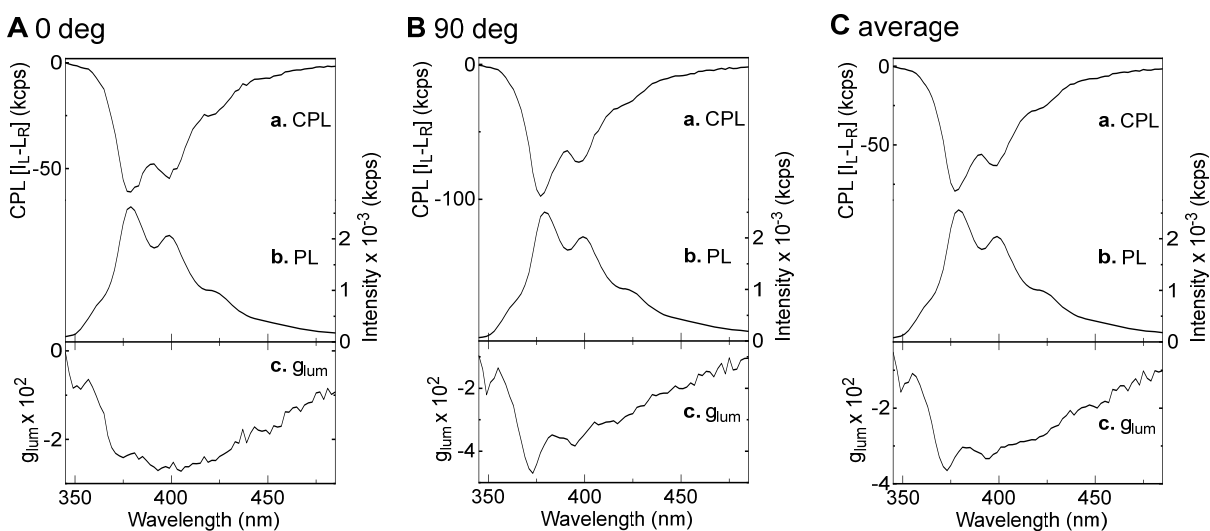
Fig. S5. CPL (a), PL (b), and g$_{lum}$ (c) spectra of **Men2Phen** film measured at 0 degrees (A) and 90 degrees (B) of the sample by irradiating the film from the *front side* of the sample and those obtained by averaging the spectra in A and B (C). [λ$_{ex}$ 260 nm]
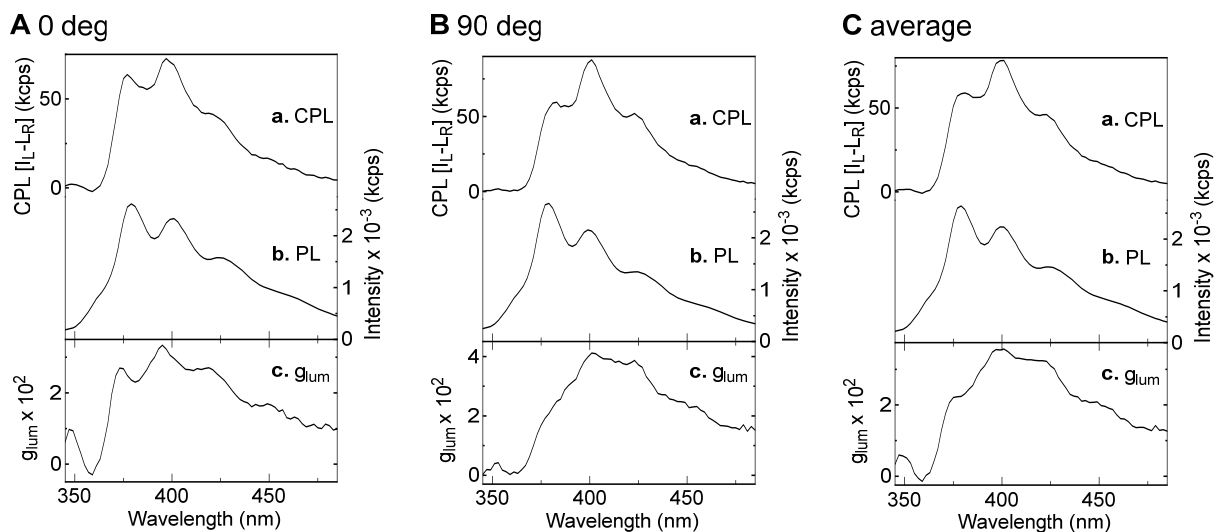
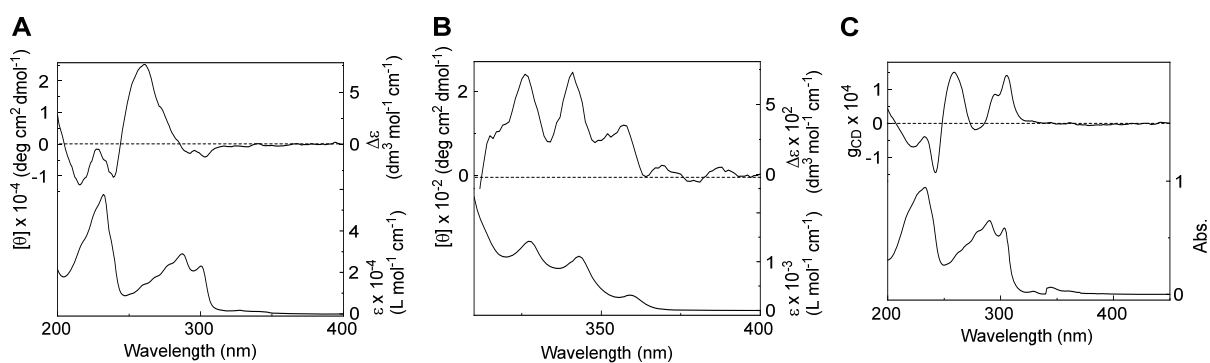**Fig. S6.** CD-UV spectra of (1*S*,2*R*,5*S*)-**Men2Phen** at 3.0 x 10^{-4} M in 1-mm cell (A) and at 6.0 x 10^{-4} M in 10-mm cell (B) in EtOH solution and in film (C). The spectra in C were obtained by averaging spectra measured at four orientations of films differing in angle by 90 degrees (Fig. S7).

Fig. S7. CPL (a), PL (b), and g$_{lum}$ (c) spectra of **MB2Phen** film measured at 0 degrees (A) and 90 degrees (B) of the sample by irradiating the film from the *back side* of the sample and those obtained by averaging the spectra in A and B (C). [λ$_{ex}$ 260 nm]
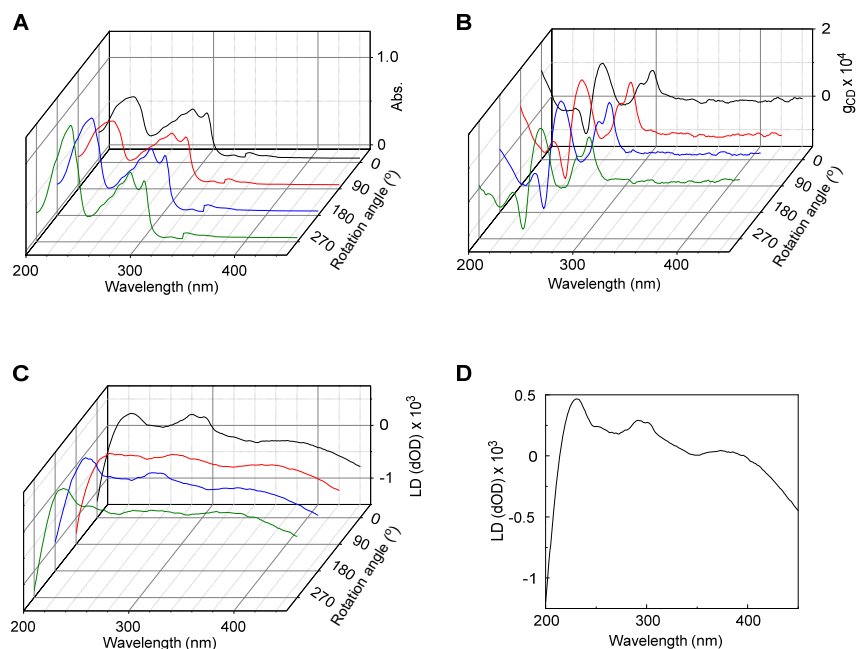
**Fig. S8.** Absorbance (A), g_{CD} (B), and LD (C) spectra of (1*S*,2*R*,5*S*)-**Men2Phen** film measured at four different angles (0, 90, 180, and 270 degrees) and averaged LD spectrum (D).
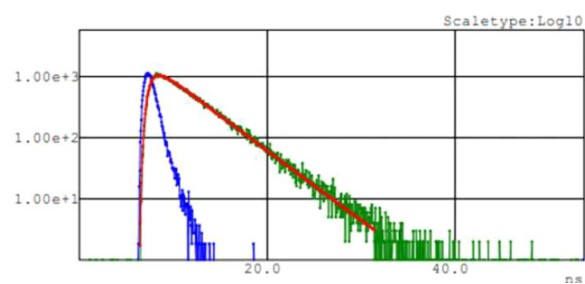

Fig. S9. CD-UV spectra of (1*S*,2*R*,5*S*)-**Men2Phen** at 3.0 x 10^{-4} M in 1-mm cell (A) and at 6.0 x 10^{-4} M in 10-mm cell (B) in EtOH solution and those in cast film (Acast film on quartz glass (solid state) obtained by averaging spectra measured at four orientations of films differing in angle by 90 degrees (Fig. S8).
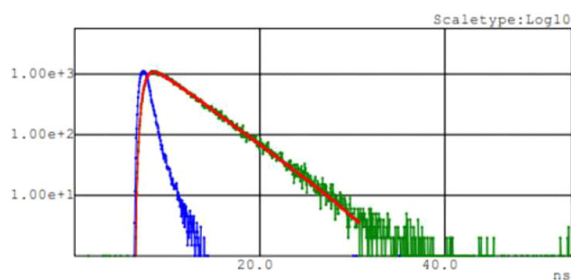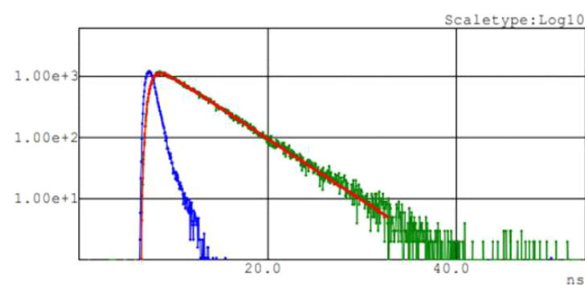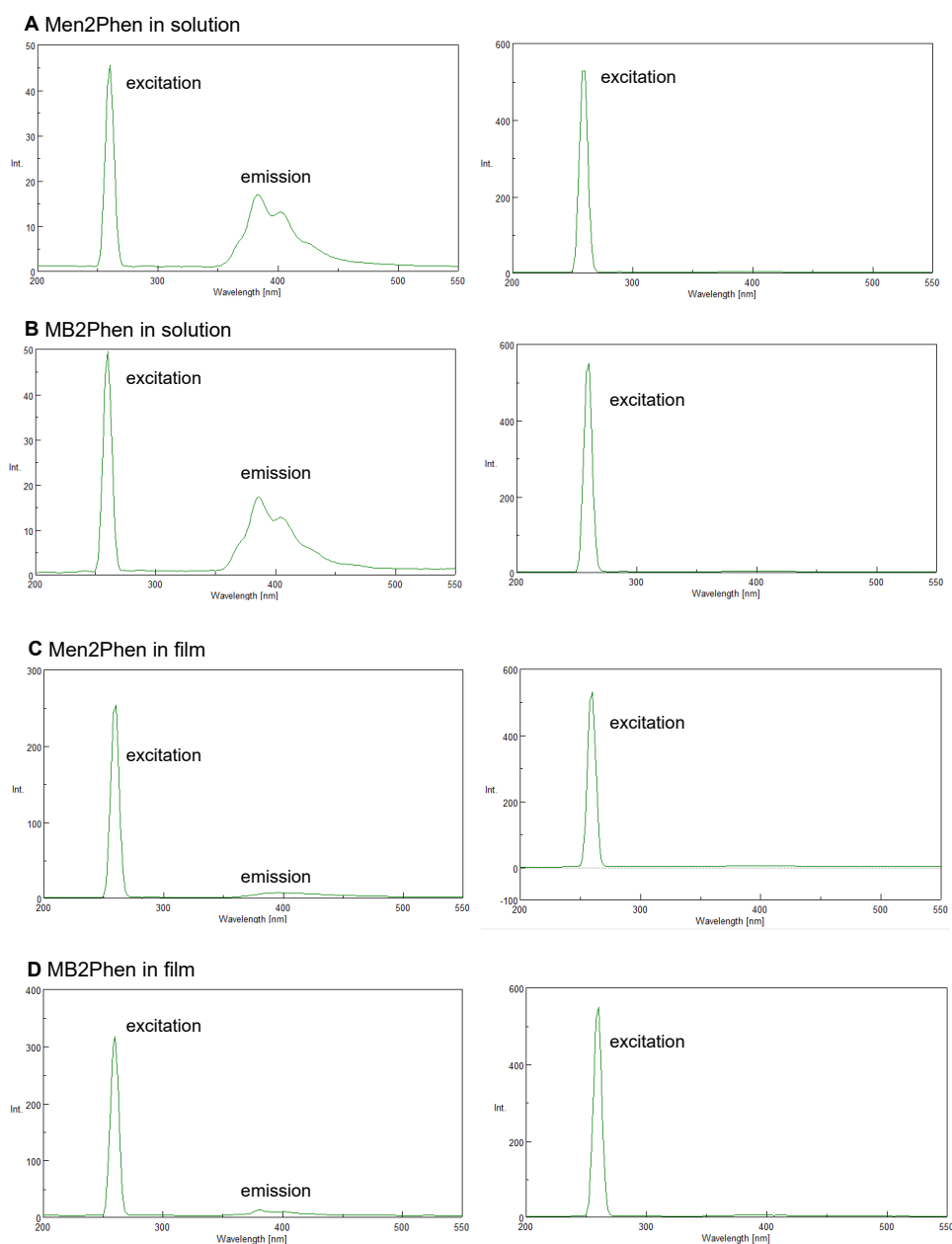
A. Men2Phen in EtOH
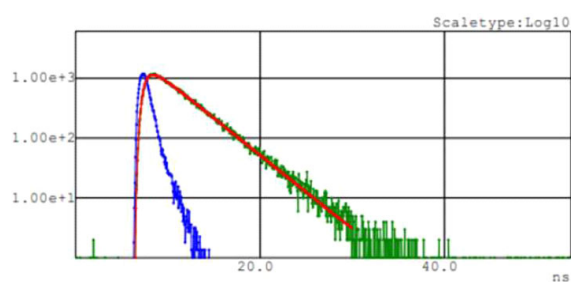
B. MB2Phen in EtOH


C. Men2Phen in film

D. MB2Phen in film

Fig. S10. Emission decay curves of **Men2Phen** in EtOH (A), **MB2Phen** in EtOH (B), **Men2Phen** in film (C), and **MB2Phen** in film (D) monitored at 380 nm. [λ_{ex} 280 nm]

**Fig. S11.** Emission spectra including excitation peaks and emission bands (left) and those with only excitation peaks (measurements with no sample) (right) of **Men2Phen** in 1,4-dioxane solution (A), **MB2Phen** in 1,4-dioxane solution (B), **Men2Phen** in film coated on quartz glass (C), and **MB2Phen** in film coated on quartz glass. [λ_{ex} 260 nm, concentration of solution samples 0.01 M, cell path 1 mm]
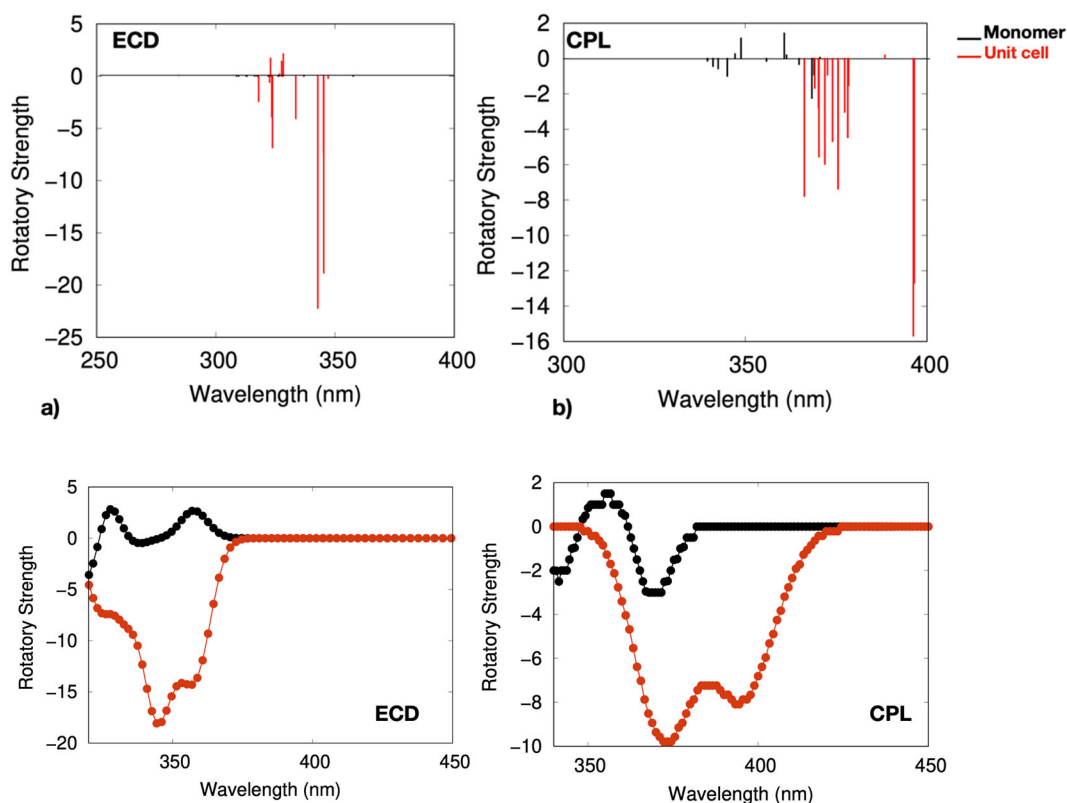
Fig. S12. Rotatory strengths vs wavelength plots (line spectra) calculated for the a) ECD and b) CPL for the Men2Phen monomer (black lines) and unit cell model (red lines) [top] as well as the corresponding fitted spectra [bottom].
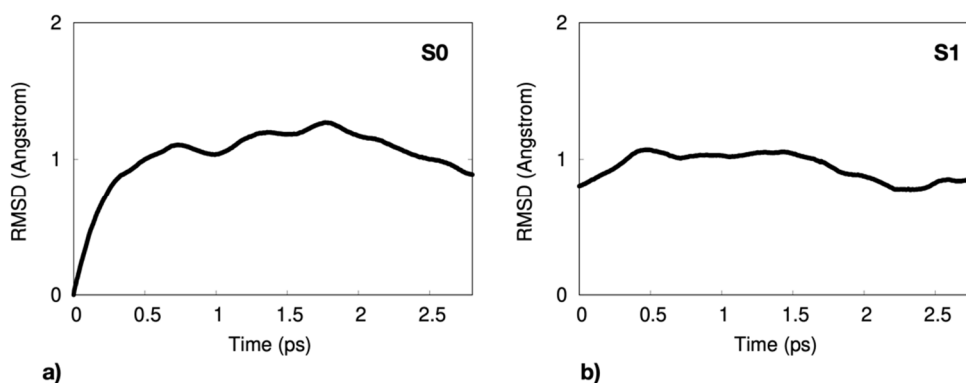
Fig. S13. RMSD values with respect to the X-ray cell structure calculated during the a) ground state AIMD trajectory and the b) first excited state AIMD trajectory.
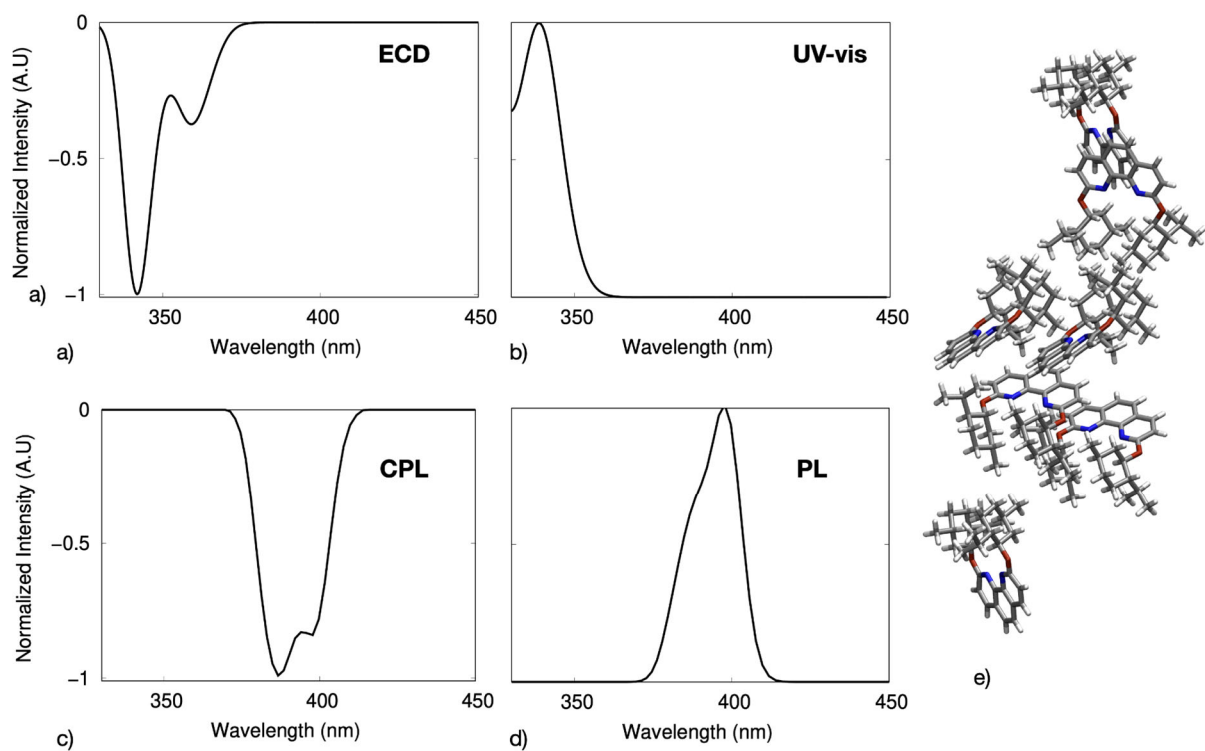
Fig. S14. CD (a), absorbance (b), CPLm (c) and total emission (PL) (d) calculated for the whole replicated coordinates (e) along a, b, and c vectors.

References

[1] S. Tanaka, K. Sato, K. Ichida, T. Abe, T. Tsubomura, T. Suzuki, K. Shinozaki, *Chem. Asian J.* **2016**, *11*, 265-273.

[2] G. M. Sheldrick, Acta Cryst., **2015**, *A71*, 3.

[3] G. M. Sheldrick, Acta Cryst., **2015**, *C71*, 3.

[4] O. V. Dolomanov, L. J. Bourhis, R. J. Gildea, J. A. K. Howard and H. Puschmann, J. Appl. Cryst., **2009**, *42*, 339.

[5] H. C. Guo, R. H. Zheng and H. J. Jiang, Org. Prep. Proced. Int., **2012**, *44*, 392.

[6] 8. Gaussian 16, Revision C01, M. J. Frisch, G. W. Trucks, H. B. Schlegel, G. E. Scuseria, M. A. Robb, J. R. Cheeseman, G. Scalmani, V. Barone, G. A. Petersson, H. Nakatsuji, X. Li, M. Caricato, A. V. Marenich, J. Bloino, B. G. Janesko, R. Gomperts, B. Mennucci, H. P. Hratchian, J. V. Ortiz, A. F. Izmaylov, J. L. Sonnenberg, D. Williams-Young, F. Ding, F. Lipparini, F. Egidi, J. Goings, B. Peng, A. Petrone, T. Henderson, D. Ranasinghe, V. G. Zakrzewski, J. Gao, N. Rega, G. Zheng, W. Liang, M. Hada, M. Ehara, K. Toyota, R. Fukuda, J. Hasegawa, M. Ishida, T. Nakajima, Y. Honda, O. Kitao, H. Nakai, T. Vreven, K. Throssell, J. A. Montgomery, Jr., J. E. Peralta, F. Ogliaro, M. J. Bearpark, J. J. Heyd, E. N. Brothers, K. N. Kudin, V. N. Staroverov, T. A. Keith, R. Kobayashi, J. Normand, K. Raghavachari, A. P. Rendell, J. C. Burant, S. S. Iyengar, J. Tomasi, M. Cossi, J. M. Millam, M. Klene, C. Adamo, R. Cammi, J. W. Ochterski, R. L. Martin, K. Morokuma, O. Farkas, J. B. Foresman, and D. J. Fox, Gaussian, Inc., Wallingford, CT, **2016**.

[7] T. D. Kuhne, M. Iannuzzi, M. Del Ben, V. V. Rybkin, P. Seewald, F. Stein, T. Laino, R. Z. Khaliullin, et al. J. Chem. Phys. **2020**, *152*, 194103.

[8] S. Nosé J. Chem. Phys. **1984**, *81*, 511.

[9] W. G. Hoover Phys. Rev. A, **1986**, *34*, 2499.

[10] S. Grimme, J. Antony, S. Ehrlich, H. A. Krieg J. Chem. Phys. **2010**, *132*, 154104.

[11] M. Fortino, G. Schifino, A. Pietropaolo Chirality, **2023**, *35*, 673.

[12] M. Fortino, A. Mattoni, A. Pietropaolo J. Mat. Chem. C, **2023**, *11*, 9135.

[13] P. Wu, A. Pietropaolo, M. Fortino, M. Bando, K. Maeda, T. Nishimura, S. Shimoda, H. Sato, N. Naga, T. Nakano Angew. Chem. Int. Ed, **2023**, *62*, e202375747.

[14] P. Wu, A. Pietropaolo, M. Fortino, S. Shimoda, K. Maeda, T. Nishimura, M. Bando, N. Naga, T. Nakano Angew. Chem. Int. Ed. **2022**, *61*, e220210556.